J Mater Sci: Mater Med (2008) 19:3081–3091
DOI 10.1007/s10856-008-3431-4

The effect of sodium-ion implantation on the properties of titanium

J. Baszkiewicz · D. Krupa · J. A. Kozubowski · B. Rajchel · M. Lewandowska-Szumieł · A. Barcz · J. W. Sobczak · A. Kosiński · A. Chróścicka

Received: 3 October 2007 / Accepted: 11 March 2008 / Published online: 5 April 2008

Abstract This paper deals with the surface modification of titanium by sodium-ion implantation and with the effect of this modification on structure, corrosion resistance, bioactivity and cytocompatibility. The Na ions were implanted with doses of 1×10^{17} and 4×10^{17} ions/cm^2 at an energy of 25 keV. The chemical composition of the surface layers formed during the implantation was examined by secondary-ion mass spectrometry (SIMS) and X-ray photoelectron spectroscopy (XPS), and their microstructure—by transmission electron microscopy (TEM). The corrosion resistance was determined by electrochemical methods in a simulated body fluid (SBF) at a temperature of 37°C, after exposure in SBF for various times. The surfaces of the samples were examined by optical microscopy, by scanning electron microscopy (SEM-EDS), and by atomic force microscopy (AFM). Biocompatibility of the modified surface was evaluated in vitro in a culture of the MG-63 cell line and human osteoblast cells. The TEM results indicate that the surface layers formed during the implantation of Na-ions are amorphous. The results of the electrochemical examinations obtained for the Na-implanted titanium samples indicate that the implantation increases corrosion resistance. Sodium-ion implantation improves bioactivity and does not reduce biocompatibility.

J. Baszkiewicz (✉) · D. Krupa · J. A. Kozubowski
Department of Materials Science and Engineering,
Warsaw University of Technology, Wołoska 141,
02-507 Warsaw, Poland
e-mail: jbasz@meil.pw.edu.pl

B. Rajchel
Institute of Nuclear Physics, Radzikowskiego 152,
31-342 Cracow, Poland

M. Lewandowska-Szumieł · A. Chróścicka
Department of Biophysics and Human Physiology,
Medical University of Warsaw, Chałubińskiego 5,
02-004 Warsaw, Poland

A. Barcz
Institute of Electron Technology, Al. Lotników 46,
02-668 Warsaw, Poland

J. W. Sobczak · A. Kosiński
Institute of Physical Chemistry, Polish Academy of Sciences,
Kasprzaka 44/52, 01-224 Warsaw, Poland

1 Introduction

The long term stability of implants depends on the surface bond between the implant and the bone tissue. Kokubo et al. [1] report that some materials have the ability to form a surface apatite layer when immersed in a simulated body fluid (SBF); through this apatite layer the material directly bonds with the living bone.

The ability of titanium surface to induce the formation of apatite is rather poor [2]. In order to improve the titanium implant integration with the bone, various surface treatments are used. Kokubo et al. [3] and Kim et al. [4] showed that the bioactivity of titanium and its alloys can be improved by NaOH– and heat treatments which result in Na_2TiO_3 being formed on the titanium surface. In SBF, Na_2TiO_3 hydrolyzes, TiOH groups form by exchanging Na^+ ions with H_3O^+ ions, and pH near the surface increases as a result of the NaOH formation. The increased number of the TiOH groups and the increased pH promote the nucleation of apatite.

An alternative method of producing surface layers with a sodium titanate content is Na^+ ion implantation. The phase composition of the surface layer formed by Na ion

implantation (with doses of $8 \times 10^{16}/4 \times 10^{17}$ Na^+/cm^2, and an ion beam energy of 20 keV) was determined by Pham et al. [5, 6]. They identified Na_2TiO_3 in the layer and found that the titanate content increases with increasing sodium dose. Pham et al. also examined [7] the bioactivity of titanium and the role played by the hydroxyl groups in the formation of hydroxyapatite at a dose of 3.2×10^{17} Na^+/cm^2 (the ion beam energy was 20 keV). It was found that, on the implanted surfaces, the concentration of the hydroxyl groups was greater than on the non-implanted surfaces. The authors suggest that the presence of these groups is not sufficient for the nucleation of calcium phosphates to take place. The necessary conditions for hydroxyapatite to form are that the solubility product should be exceeded and the porosity should be optimal. How the surface morphology varies with the sodium dose was reported by Cai et al. [8]. They observed that the greatest increase of the surface roughness occurred with a dose of 1×10^{17} Na^+/cm^2. Maitz et al. [9–11], on the other hand, examined the effect of sodium ion implantation on the biocompatibility of titanium. Their results show that, on the implanted surfaces, the cell growth is irregular.

Classical implantation is a line-of-sight process. In plasma immersion ion implantation (PIII), all surfaces of the target are implanted simultaneously. Maitz et al. [11] compare the bioactivity and biocompatibility after the surface modification using three different methods, namely classical ion implantation, PIII and alkali treatment.

The increase of the bioactivity of titanium can also be achieved by calcium ion implantation. Hanawa et al. [12, 13] have found that calcium ion implantation improves the ability of titanium to promote the formation of calcium phosphate. Examinations of the chemical composition of the surface layers formed during the calcium ion implantation show that the implanted ions occur in these layers in the form of calcium oxide and calcium titaniate. In in vivo examinations [14], calcium implantation appeared to be advantageous for the growth of bone tissues. Examination of the corrosion resistance of calcium implanted titanium show that pitting corrosion occurs during polarization [15].

If titanium and its alloys are to be used for implants in the human body, it is crucial that the surface modification should not degrade their corrosion resistance.

Therefore, the present study was aimed at examining the effect of sodium-ion implantation on the corrosion resistance of titanium.

2 Materials and methods

The material examined was titanium grade 2. The samples were in the form of discs with a diameter of 14mm for corrosion examination and a diameter of 6mm for biological examination. The samples were polished mechanically on one side to a mirror finish and then implanted with sodium ions using doses of 1×10^{17} ions/cm^2 and 4×10^{17} ions/cm^2 at a beam energy of 25 keV. During the implantation, the temperature did not exceed 40°C. The vacuum in the target chamber was about 10^{-6} Pa. The conditions under which the implantation was carried out were selected in order to maximize the sodium concentration on the surface. Sodium profiles were calculated using the TRIM code [16] and corrected for the sputtering effect that takes place during the implantation. At an energy of 25 keV and doses higher than 4×10^{17} Na^+/cm^2, the depth of sputtering is so great that it is not possible to obtain concentrations greater than approximately 50 at.%.

The implantation was carried out at the Institute of Nuclear Physics in Cracow, Poland.

The surface layers were analyzed using the following methods:

- Transmission electron microscopy (TEM): structural examinations were made with a Philips EM-300 TEM. The test samples were cut by the electrospark method and then thinned on the non-implanted surface until a perforation occurred.
- Secondary-ion mass spectrometry (SIMS): profiling was carried out using a Cameca IMS 6F instrument with a cesium primary beam at an impact energy of 6 keV.
- X-ray photoelectron spectroscopy (XPS): investigations were performed using a Microlab 350 spectrometer with an X-ray source. A Mg Kα radiation source operated at a power of 300 W (15 kV, 20 mA) was applied (1,253.6 eV). The binding energy scale was calibrated by the C 1s peak at 285.00 eV. Quantification was carried out using the standard Scofield sensitivity factors and the transmission function of the spectrometer provided by the producer.
- Scanning electron microscopy (SEM) (model S 3500-L, Hitachi) with EDS (Energy-dispersive X-ray spectroscopy).
- Atomic force microscopy (AFM) (Multi Mode Nanoscope IIIA DI Veeco).
- Optical microscopy.

Corrosion resistance was examined in a non-deaerated simulated body fluid (SBF) at a temperature of 37°C. The chemical composition of the SBF is given in Table 1.

Table 1 Chemical composition of the simulated body fluid (SBF) (mM)

Na^+	K^+	Ca^{2+}	Mg^{2+}	Cl^-	HCO_3^-	HPO_4^{2-}	SO_4^{2-}
142	5	2.5	1.5	147.8	4.2	1	0.5

The following techniques were employed:

- Stern's method (linear polarization method). Measurements were begun at a potential of 20 mV, lower than the corrosion potential E_{corr}, and then the potential was increased in the anodic direction until a potential higher by 20 mV than E_{corr} was achieved. The polarization resistance R_p was calculated using the least square method.
- Electrode impedance spectroscopy (EIS). The impedance tests were conducted at the corrosion potential (E_{corr}) by applying a sinusoidal potential signal of ±20 mV within a frequency range of 0.01–10 kHz. The impedance spectra were analyzed using the EQUVCRT program [17].
- The polarization curves having been measured, the samples were polarized in the anodic direction beginning from a potential of –600 mV up to a potential of 5,000 mV at a scan rate of 20 mV/min.

The reference electrode was a saturated calomel electrode, and the counter electrode was made of platinum.

Prior to the measurements, the samples were exposed to the test conditions for 13, 181, 733 and 2,100 h. The aim of the 13 h exposure was to allow the corrosion potential (E_{corr}) to stabilize. The long-term exposures were used for examining how the formation of the phosphate layer and the changes in the properties of oxide layer affect the corrosion resistance of titanium.

2.1 Cytocompatibility study in vitro

The influence of the applied surface modification on cells behaviour in vitro was tested in a culture of the MG-63 cell line (human osteosarcoma cell line, ATCC collection) and human osteoblast cells. The cells were seeded at a density of 2,000/well (i.e. 6,500 cells/cm^2) on the surface of the samples and on a surface of modified polystyrene (the bottom of a culture dish), which served as a control. The cells were cultured under standard conditions (5% CO_2, 95% humidity) in a culture medium based on DMEM (GIBCO BRL) enriched with 10% heat-inactivated fetal calf serum (GIBCO BRL), an antibiotic-antimycotic (GIBCO BRL), L-glutamine (GIBCO BRL) and 100 μM L-ascorbic acid 2-phosphate (SIGMA). After 24 h, the medium was replaced by the same medium supplemented with dexamethasone (10 mM).

After 2 days, the cells in contact with the investigated titanium samples were subjected to morphological observations with a scanning electron microscope (SEM). After 8 days, the viability of the cells was determined by means of the XTT assay used in toxicology. That test is based on the capacity of mitochondrial dehydrogenase enzymes present in living cells to convert the XTT substrate (2,3-bis(2-methoxy-4-nitro-5-sulfophenyl)-5-[(phenyloamino) carboxyl]-2Htetrazolium hydroxide) into a water-soluble formazan product. The final product of the reaction was measured with an ELISA reader at 450 nm. At least six samples of each type were tested, and the experiments were performed twice.

3 Results

3.1 TEM results

In its initial state, titanium has a polycrystalline structure, contains dislocations and, within large (above 1 μm) grains, has a great number of subgrains separated by blurred boundaries [15]. Implantation of sodium ions results in the formation of an amorphous layer on the surface.

3.2 SIMS results

The measured depth profiles of the elements present in the surface layer are shown in Fig. 1a. The measured sodium-depth penetration is about 100 nm for a dose of 1×10^{17} Na^+/cm^2, whereas for a dose of 4×10^{17} Na^+/cm^2, it is about 200 nm, greater than theoretical (100 nm) [18]. During the implantation, the surface layers were enriched with oxygen. The oxygen-penetration depth was smaller with the lower sodium dose. The anodic polarization of the sodium-implanted titanium does not essentially alter the SIMS profile—the titanium surface undergoes a slight oxidation (Fig. 1b).

3.3 XPS results

The XPS results obtained for Ti implanted with a dose of 4×10^{17} Na^+/cm^2 (Table 2) show the variation of the chemical composition of the implanted layer as a function of the etching time. As the etching time increases, the concentration of oxygen and carbon decreases, whereas the share of titanium increases. Deconvoluting the XPS spectra of the sodium and oxygen present in the implanted layers and determining their bonding energies show that the implanted sodium is bonded, probably with oxygen. To the depth reached by the first 20 scans, titanium exists as Ti^{4+} (probably as TiO_2) but, after that, it exists as metallic titanium.

3.4 AFM results

The morphology of the surface was examined before and after exposure in SBF. The AFM images of the surface of the non-implanted and sodium-implanted titanium are shown in Fig. 2. During sodium-ion implantation, the

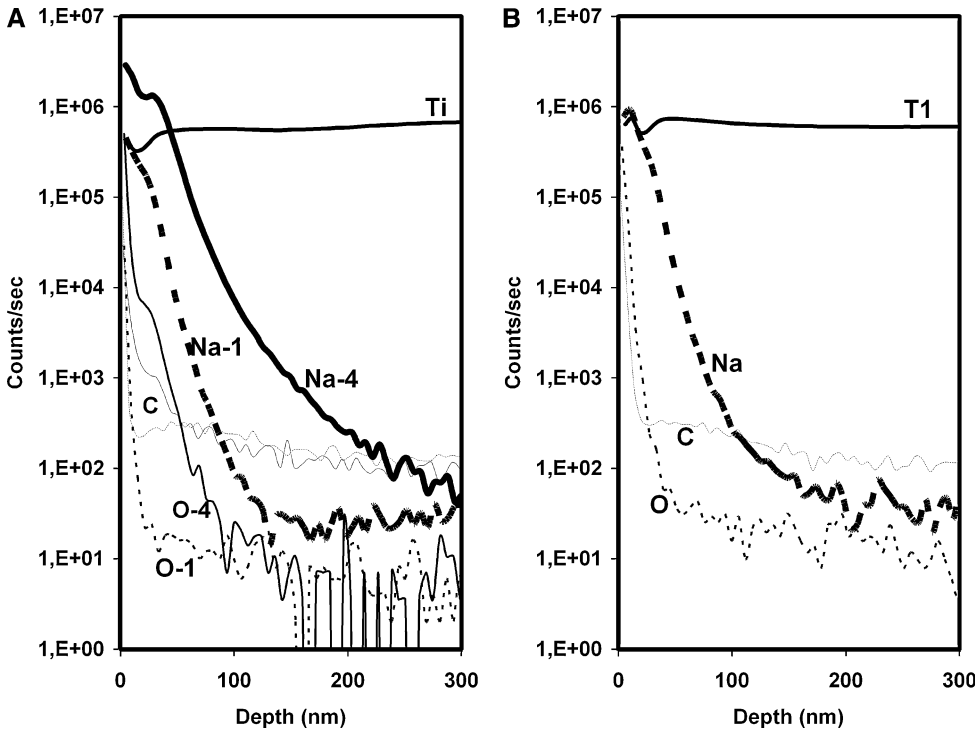

Fig. 1 Depth profiles of the oxygen, carbon, titanium and sodium. (**a**) titanium implanted with doses of 1×10^{17} Na^+/cm^2 and 4×10^{17} Na^+/cm^{2-} in its initial state, (**b**) titanium implanted with a dose of 1×10^{17} Na^+/cm^2, after electrochemical investigation. Na-1, O-1—sodium and oxygen depth profiles for the dose of $1 \times 10^{17}Na^+/cm^2$, Na-4, O-4—sodium and oxygen depth profiles for the dose of $4 \times 10^{17}Na^+/cm^2$

Table 2 Relative concentrations of the elements in the surface layer of sodium-implanted Ti with a dose of $4 \times 10^{17}Na^+/cm^2$

Etching time (s)	Relative concentration (at.%)			
	Na	O	C	Ti
0	14.7	50.5	19.5	13.8
100	31.5	46.7	3.42	17.4
5,918	39.5	32.6	2.92	23.0

surface undergoes ion-etching and its morphology changes. Surface images after exposure in SBF are shown in Fig. 3. The variations of the surface roughness after sodium-ion implantation and after 7 days exposure in SBF are shown in Fig. 4.

3.5 Corrosion examinations

Figures 5 and 6 show the results of DC examinations. Figure 5 shows the effect of the sodium-ion dose and time of exposure in SBF on polarization resistance (R_p). The anodic polarization curves are shown in Fig. 6. The effect of exposure time on the average value of the anodic current densities measured within the in vivo potential range for titanium (210−310 mV) [19] is shown in Table 3.

3.5.1 Non-implanted titanium

Results obtained for non-implanted titanium indicate that the longer the exposure time, the higher the corrosion resistance. This effect is visible in Fig. 5—the polarization resistance R_p increases with increasing exposure time. After 2,100 h exposure in SBF, the polarization resistance of the non-implanted titanium is the highest but also has the highest dispersion. The advantageous effect of prolonged exposure time on the shape of the anodic polarization curves can be seen in Fig. 6a. The polarization curves within the potential range of −200 to 900 mV show a decrease of the anodic current density compared with that measured in the samples exposed for 13 h (Fig. 6a). Above a potential of 2.5 V, the current density gradually increases in all samples, its value being higher in the longer-exposed samples.

3.5.2 Sodium-ion-implanted titanium

The values of polarization resistance R_p determined for the sodium-implanted titanium after 13 h exposure suggest that the implantation improves the corrosion resistance of titanium (Fig. 5). This effect is more pronounced for the sodium dose of 1×10^{17} Na^+/cm^2. After prolonged exposure time (733 h) the values of polarization resistance for non-implanted and sodium-implanted titanium are almost the same.

The effect of sodium-ion implantation on the anodic polarization curves of titanium can be seen in Fig. 6. Comparing the anodic polarization curves obtained after 13 h exposure in SBF for non-implanted titanium and sodium implanted samples, we can see that implanted

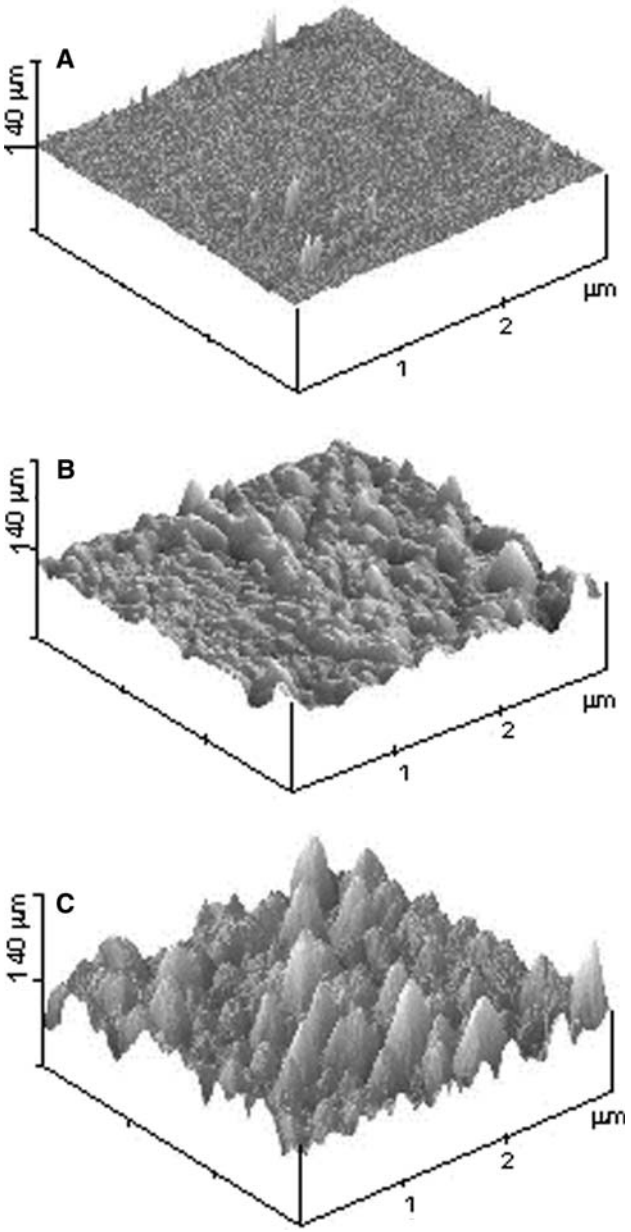

Fig. 2 Surface morphologies of titanium: (**a**) non-implanted, (**b**) after sodium-ion implantation with a dose of $1 \times 10^{17} Na^+/cm^2$, (**c**) after sodium-ion implantation with a dose of 4×10^{17} Na^+/cm^2

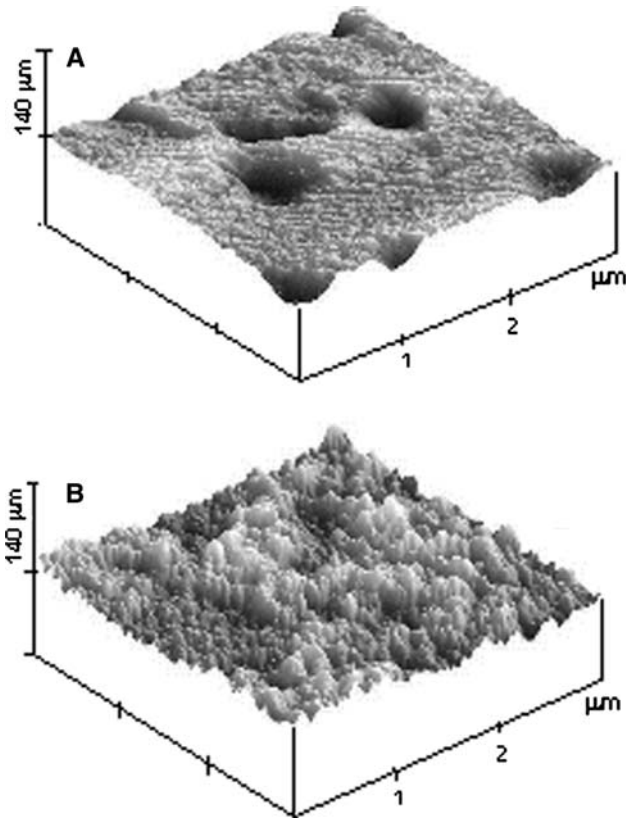

Fig. 3 Surface morphologies of titanium after 7 days' exposure in SBF: (**a**) non-implanted, (**b**) sodium-ion implanted with a dose of 4×10^{17} Na^+/cm^2

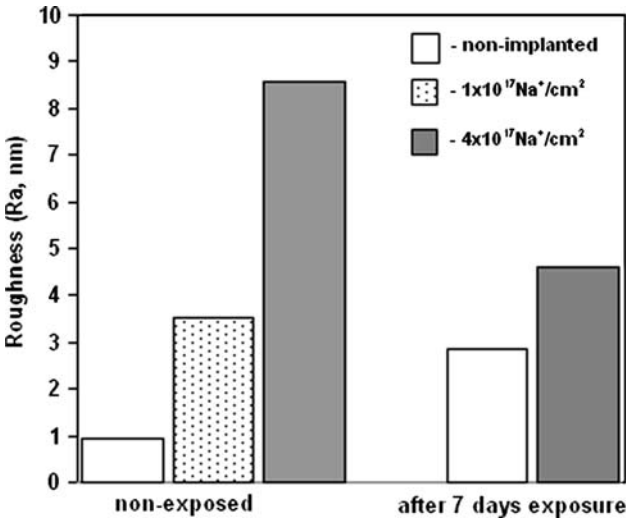

Fig. 4 Surface roughness of titanium and sodium-implanted titanium before and after 7 days' exposure in SBF

samples have lower anodic current densities. Furthermore, in the potential range between −200 and +400 mV, the specimens implanted with a dose of 1×10^{17} Na^+/cm^2 have the lowest anodic current densities. On the other hand, the polarization curves obtained after long periods of exposure are similar for both the non-implanted and the implanted samples. With an increase of exposure time, one can observe, within the potential range of −200 to 900 mV, a decrease of the anodic current density compared to that measured in the samples exposed for just 13 h (Fig. 6b and c).

By comparing average anodic current densities within the potential range 210–310 mV (Table 3), we find that, as the exposure time increases, the anodic current decreases. After long-term exposure (2,100 h), the values of anodic

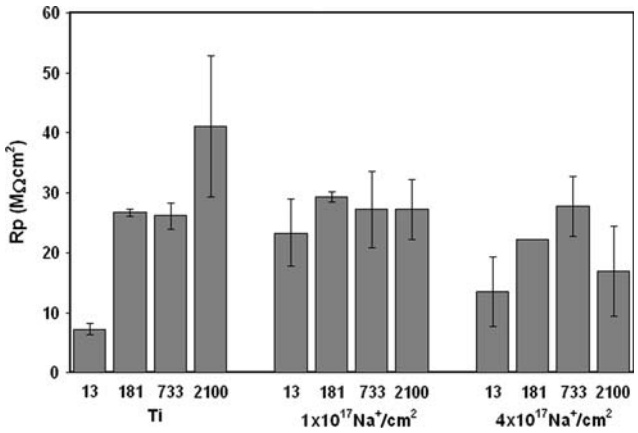

Fig. 5 Polarization resistance for titanium and sodium-ion implanted titanium as a function of exposure times in SBF (time in hours)

current densities are almost the same for the non-implanted and sodium-implanted titanium with a dose of 1×10^{17} Na^+/cm^2, but for the titanium implanted with the higher sodium dose, the anodic current density is twice as great as that for the non-implanted.

3.6 Impedance measurements

The results of the impedance examinations are shown in Fig. 7. The Bode diagrams shown in Fig. 7a can be interpreted by using a simple Randles equivalent circuit $R(R_bQ_b)$ where R represents electrolyte resistance, R_b resistance, and Q_b the constant phase element of the barrier layer. The Bode diagrams shown in Fig 7c can be interpreted using equivalent circuit $R(R_pQ_p)(R_bQ_b)$ where R_p represents resistance, and Q_p the constant phase element of the porous layer. Since the values of the resistance of the barrier layer R_b calculated from these models were widely spread, the simplified equivalent models RQ_b or $R(R_pQ_p)Q_b$ were used.

The impedance spectra obtained for non-implanted titanium (Fig. 7a) indicate that the surface oxide (passive) layer on the titanium has a capacitive character and does not change during exposure in SBF.

Sodium-ion implantation with a dose of 4×10^{17} Na^+/cm^2 alters the character of the spectrum and hence needs to be interpreted using an equivalent circuit with two time constants (Fig. 7c). The surface layer formed on the sodium-implanted titanium with a dose of 4×10^{17} Na^+/cm^2 is composed of an outer, porous layer and an inner, barrier layer. During exposure in SBF, the character of the oxide layers does not change, but its parameters do. The impedance spectra for titanium implanted with the dose of 1×10^{17} Na^+/cm^2 (Fig. 7b) obtained after 13 and 181 h exposure in SBF can be interpreted using equivalent circuits to those for the non-implanted titanium, but the spectra obtained after more prolonged exposure must be interpreted using an equivalent circuit to that for the titanium implanted with the higher sodium dose.

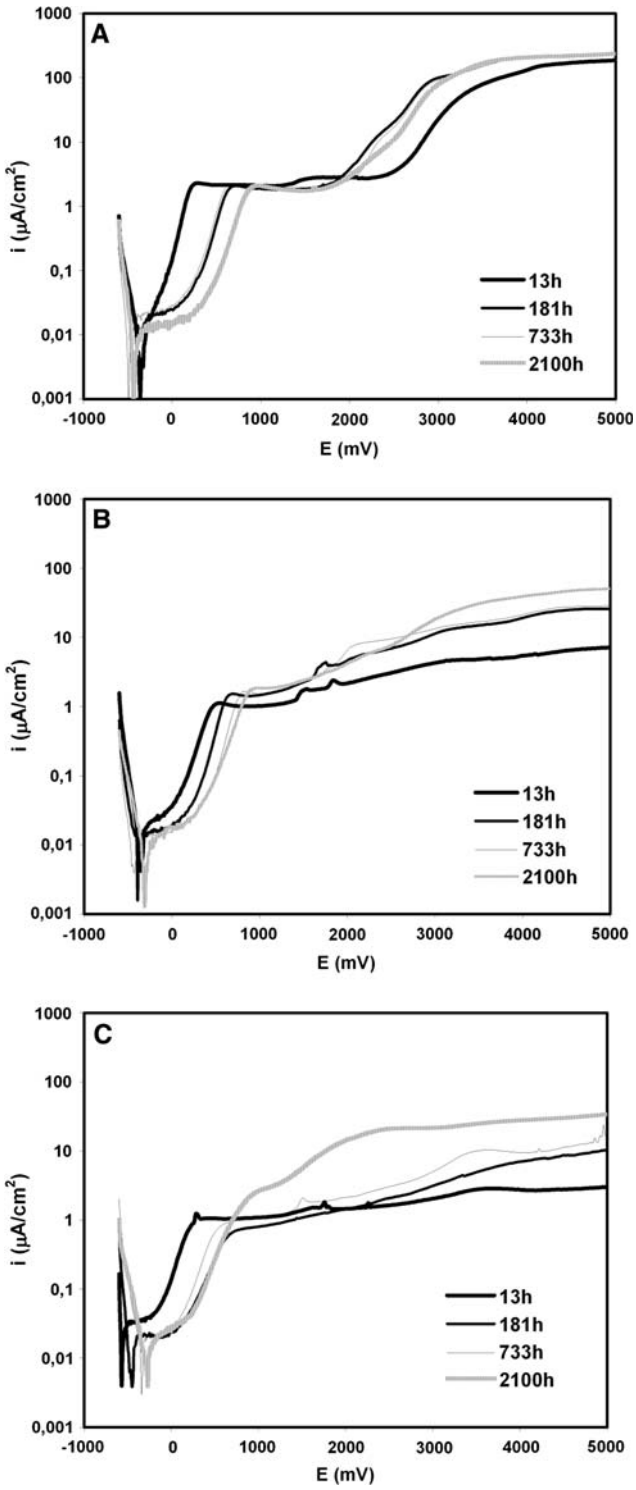

Fig. 6 Anodic polarization curves obtained after various times of exposure in SBF, for non-implanted titanium (**a**), and sodium-implanted titanium with doses of 1×10^{17} Na^+/cm^2 (**b**), and $4 \times 10^{17}Na^+/cm^2$ (**c**)

Table 3 Anodic current densities within potential range 210–310 mV for titanium and sodium-implanted titanium after various times of exposure in SBF

Exposure time (h)	i (μA/cm^2)		
	Ti	Ti 1 × 10^{17} Na$^+$/cm^2	Ti 4 × 10^{17} Na$^+$/cm^2
13	2.1	0.19	0.97
181	0.062	0.047	0.058
733	0.076	0.027	0.11
2,100	0.024	0.025	0.050

3.7 Bioactivity examinations

After immersion in SBF, phosphate layers formed on the surface of all examined specimens (Fig. 8). Initially they had the character of islands. With prolongation of exposure time, the amount of phosphates increased and after 2,100 h a compact and continuous layer was observed on the surfaces both of the titanium implanted with a dose of 1 × 10^{17} Na$^+$/cm^2 and that implanted with a dose of 4 × 10^{17} Na$^+$/cm^2 (Fig. 8c). The phosphates that formed on the surface of the non-implanted titanium specimens did not form a compact layer, but only precipitates (Fig. 9a). The calcium-to-phosphorus ratio for all types of specimens increased with an increase in the exposure time (Fig. 10). After 2,100 h exposure, the [Ca]/[P] ratio for phosphates formed on the surface of the sodium-implanted specimens was about 1.7 (1.66 for hydroxyapatite), while for phosphates formed on the surface of the non-implanted specimens, it was about 2.

3.8 Biocompatibility examination

The results of the XTT viability assay are presented in Fig. 11. The results obtained in the control (i.e., the cells maintained on the standard tissue culture surface) are taken as a reference, and thus the viability of the cells cultured on the surface of the non-implanted titanium as well as that of the cells in contact with the sodium implanted titanium is expressed as a percent of the viability of the cells in the control. Based on our experiments with human osteoblast cells (Fig. 11a), we can say that that the viability of the cells on the surface of the titanium specimens is statistically significantly lower than that on the control surface. On the other hand, there were no statistically significant differences in viability between those in contact with non-implanted and those in contact with the sodium-implanted titanium. There was a statistically significant increase in viability for the MG63 cells (Fig. 11b) cultured in contact with the sodium-implanted

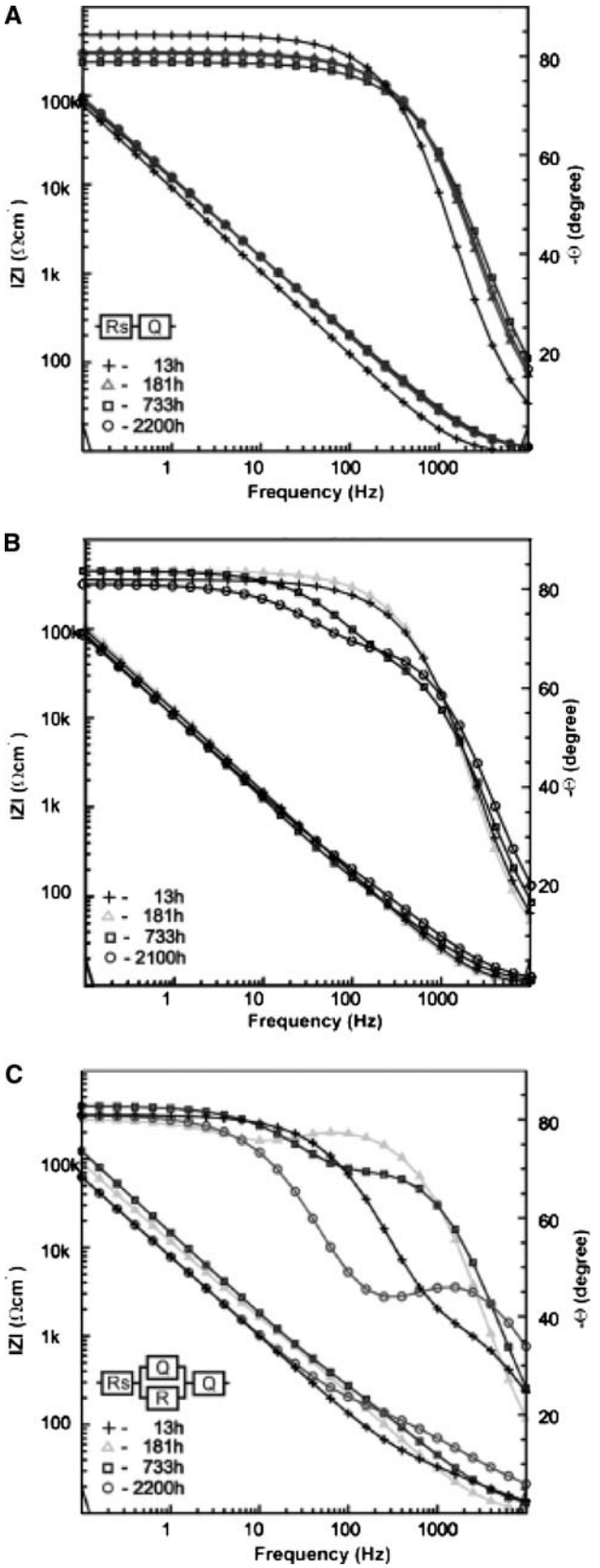

Fig. 7 Bode plots after various times of exposure in SBF for non-implanted titanium (**a**), and sodium-implanted titanium with doses of 1 × 10^{17} Na$^+$/cm^2 (**b**) and 4 × 10^{17}Na$^+$/cm^2 (**c**)

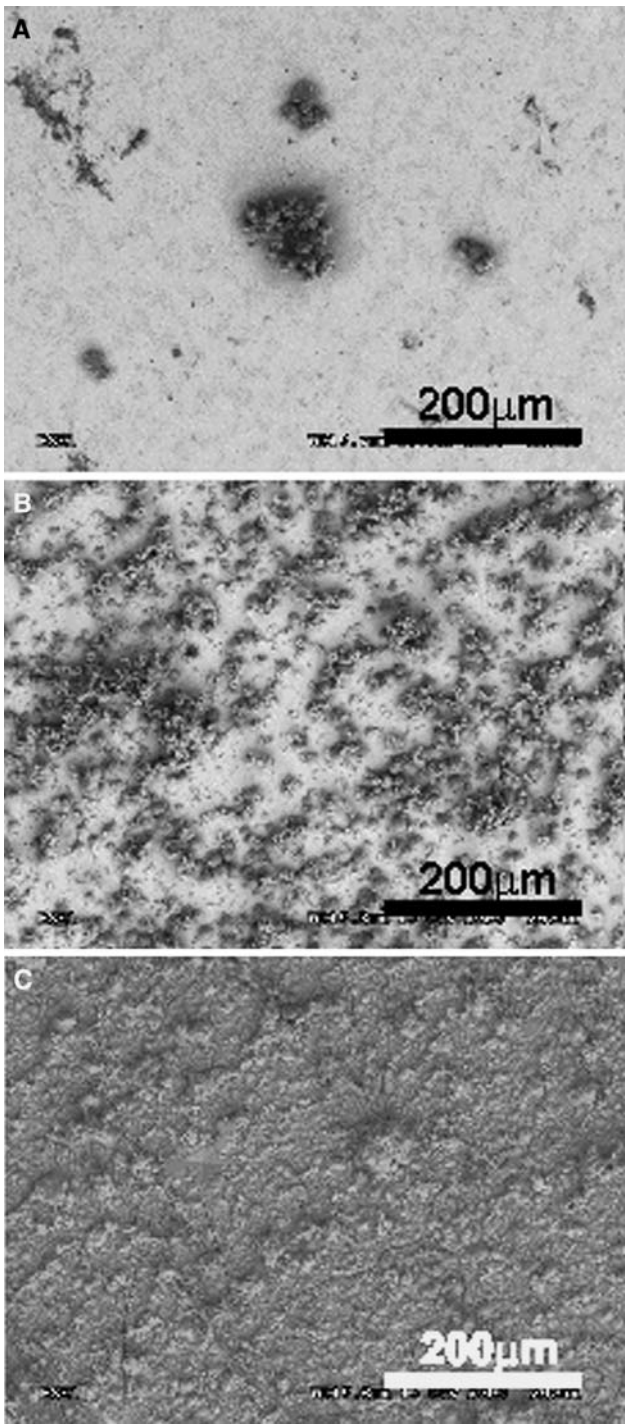

Fig. 8 Scanning electron micrographs of the surface of sodium-implanted titanium with a dose of 1×10^{17} Na^+/cm^2 after exposure in SBF: (**a**) 171 h, (**b**) 733 h, (**c**) 2,100 h

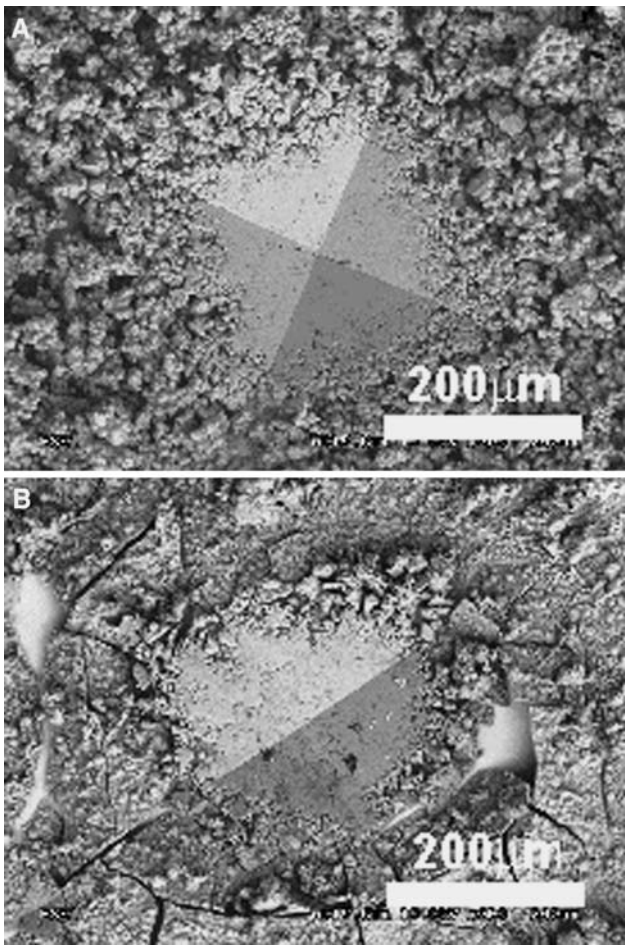

Fig. 9 Scanning electron micrographs of the surface after 2,100 h exposure in SBF and after Rockwell micro-hardness test with a load of 49N. (**a**) non-implanted, (**b**) sodium-implanted titanium

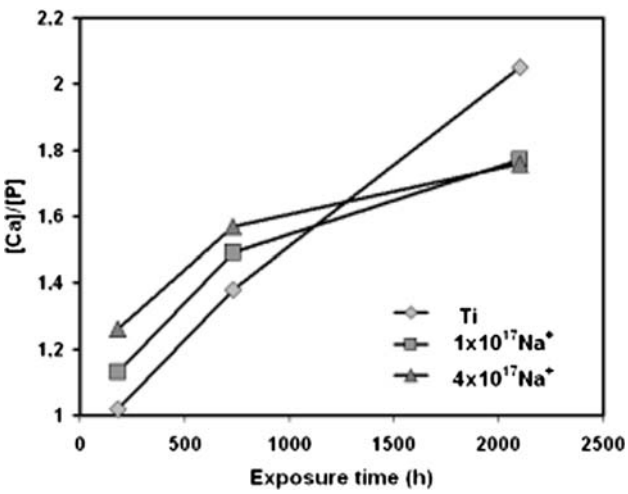

Fig. 10 [Ca]/[P] ratio as a function of exposure time and sodium dose

titanium with a dose $4 \times 10^{17}/cm^2$ in comparison to those in contact with the non-implanted titanium. We did not observe any statistically significant differences in cell viability between the sodium-implanted titanium with a dose of 1×10^{17} Na^+/cm^2 and the non-implanted titanium.

The cells cultured on the surface of the sodium-implanted titanium displayed good spreading (Fig. 12), as visualized by SEM.

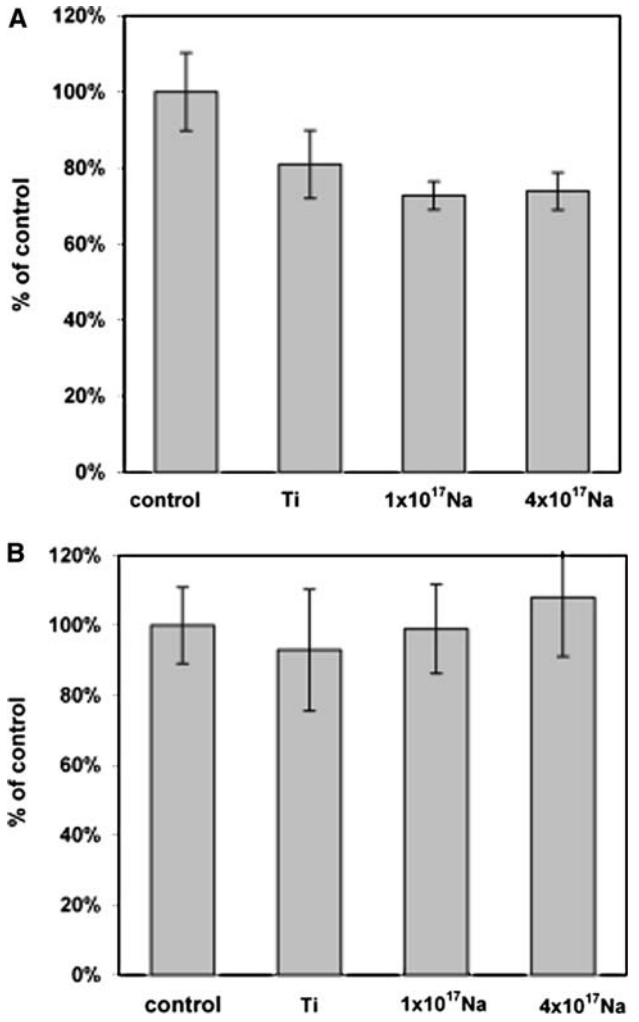

Fig. 11 Results of the XTT assay. (**a**) human osteoblast, (**b**) MG-63 cell

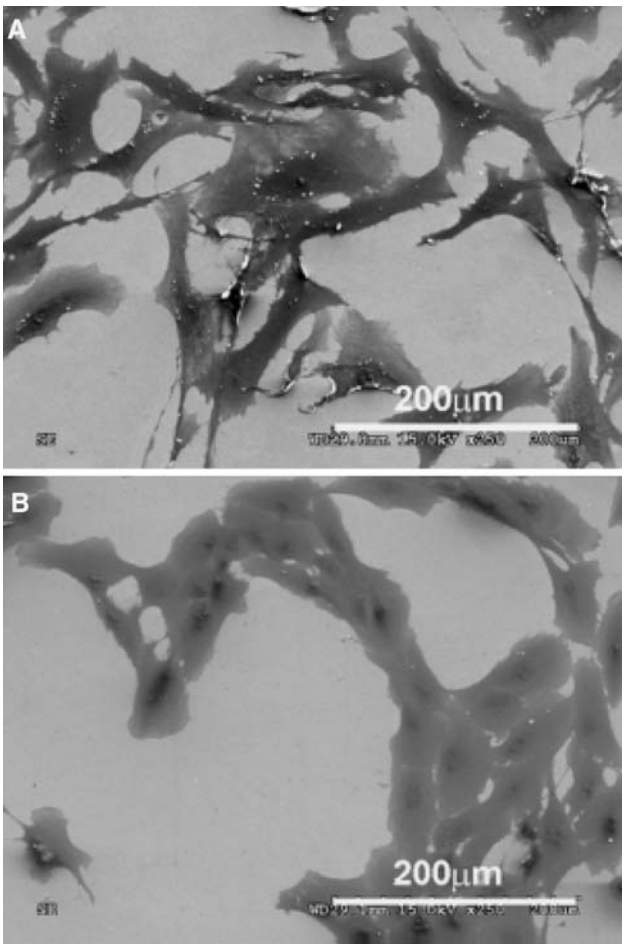

Fig. 12 Scanning electron micrographs of cells cultured on the surface of sodium-ion implanted titanium with a dose 4×10^{17} Na^+/cm^2: (**a**) human osteoblast, (**b**) MG-63 cell

4 Discussion

Sodium does not form stable solutions or intermetallic compounds with titanium [20]. It is an active metal, and its presence in the surface layer ought to have a negative influence on the corrosion resistance of titanium. However, the results presented here show that sodium-ion implantation actually increases the corrosion resistance of titanium. This change in corrosion resistance can be attributed to the changes in the morphology, structure, and chemical composition of the surface layer.

Surface etching during the sodium-ion implantation of titanium produces an increase in surface area (Fig. 2). A similar effect has been observed by Pham et al. [21] and Cai et al. [8]. A change in surface roughness can cause a change in corrosion resistance. Comparing the surface image of specimens implanted with different doses of sodium (Fig. 2), we can see that there is greater surface expansion for those implanted with a dose of 4×10^{17} Na^+/cm^2. Based on Fig. 2c and assuming that, on a surface of 9 μm^2, about 100 cones with a height of 100 nm were produced as a result of sodium ion-implantation with a dose of 4×10^{17} Na^+/cm^2, we can calculate the actual surface area of the specimen, revealing the increase of surface area of the sample during implantation to have been approximately 15%. The effect of increased surface roughness on corrosion resistance has been investigated by Lange et al. [22] and Kirbs et al. [23, 24]. Those studies indicate that an increase in roughness is associated with a increase in the corrosion current and a decrease in the polarization resistance of titanium. This effect was not observed on our sodium-implanted titanium specimens. Despite an increase in the actual specimen surface area (by about 15%), the corrosion resistance of the titanium after sodium-ion implantation was greater than that for non-implanted titanium. The aforementioned authors [22–24] did not make allowance for the changes in the chemical composition and structure of the surface layers that take place during surface preparation.

The observed increase in corrosion resistance may be attributed to the formation of an amorphous layer during implantation. Titanium is a metal whose high corrosion resistance is the result of the presence of a passive layer, and in general, it is known that the formation of amorphous layers on the surface of metals whose corrosion resistance depends on passive layers tends to produce increased corrosion resistance [25–27].

During sodium-ion implantation, an amorphous surface layer with a high concentration of sodium was formed. The theoretical sodium concentration in this layer for a dose of 1×10^{17} Na^+/cm^2 would be about 15%, and for a dose of 4×10^{17} Na^+/cm^2, about 50%. XPS examinations show that actual sodium concentrations are lower than the theoretical (Table 2). From the deconvolution of the Na1s spectra obtained for the sodium-implanted titanium, we see that the binding energy of the sodium is about 1072.3–1073 eV, which suggests that, in the outer part of the implanted layer, sodium is bonded with oxygen. Because the depth of the oxygen penetration is lower than the depth of penetration of the sodium (Fig. 1), the sodium in the deeper part of the implanted layer is non-bonded.

The corrosion resistance of sodium implanted titanium is thus dependent primarily on two opposing factors: passive layer formation (beneficial) and the presence of sodium in the surface layer (adverse).

Specimens implanted with a lower dose (1×10^{17} Na^+/cm^2), which have smaller concentration of sodium in their surface layers, show a threefold increase in polarization resistance (Fig. 5) and a nearly tenfold decrease in anodic current density (Table 3). This effect can be attributed to the presence of an amorphous layer, covered with a passive layer, which has better protective properties than passive layers on polycrystalline material. The lesser increase in corrosion resistance for the titanium implanted with a higher sodium dose (4×10^{17} Na^+/cm^2) can be ascribed to the higher concentration of sodium in its surface layers.

Long-term exposure in SBF results in changes in corrosion resistance. An increase in the corrosion resistance of titanium during exposure in SBF has been observed in a number of studies [15, 26–29]. The highest increase in corrosion resistance during exposure in SBF has been observed for specimens of titanium in its initial state. This increase in corrosion resistance is manifested by an increasing polarization resistance and by an almost hundredfold decrease in anodic current density (Table 3). For non-implanted specimens exposed for 2,100 h in SBF, a wide dispersion of measured results has been observed, probably due to the presence of phosphate layers on the surface of the specimens. Prolongation of the exposure time of sodium-implanted specimens also has a beneficial effect on their corrosion resistance. In the case of the specimens implanted with a dose of 1×10^{17} Na^+/cm^2, polarization resistance practically does not change (Fig. 5), but the anodic current density is seven times lower than in samples exposed for 13 h (Table 3). The polarization resistance of specimens implanted with a dose of 4×10^{17} Na^+/cm^2 initially rises as exposure time increases, but after 2,100 h exposure, its value is nearly the same as after 13 h of exposure. The anodic current density for these samples decreases during exposure about 20 times, compared to its value after 13 h of exposure.

Taking as a criterion the results of the DC examinations, we can arrange investigated samples in order of diminishing corrosion resistance as follows:

- after 13 h exposure in SBF Ti (1×10^{17} Na^+/cm^2) > Ti (4×10^{17} Na^+/cm^2) > Ti
- after 2,100 h exposure in SBF Ti ≥ Ti (1×10^{17} Na^+/cm^2) > Ti (4×10^{17} Na^+/cm^2)

Comparing the corrosion resistance of non-modified titanium with that of sodium-implanted titanium, we can say that sodium implantation with a dose 1×10^{17} Na^+/cm^2 produces an increase in corrosion resistance after 13 h of exposure and does not decrease corrosion resistance even after 2,100 h exposure in SBF. On the other hand, sodium implantation with a dose of 4×10^{17} Na^+/cm^2 also produces increased corrosion resistance after 13 h of exposure, but after 2,100 h of exposure the corrosion resistance of titanium treated in this way is lower than that for non-implanted titanium.

Sodium-ion implantation results in an etching of the titanium surface, and hence an increase in its roughness (Figs. 2, 4). From point of view of titanium's use as a metallic biomaterial, such surface development is desirable. Surfaces with a roughness on the order of 10 nm or less support the adsorption of small organic particles and inorganic ions [30]. As a result of exposure in SBF, the surface morphology of both non-implanted titanium and sodium-implanted titanium undergoes a change. This effect can be seen by a comparison of the surface images shown in Figs. 2 and 3. The surface of non-implanted titanium undergoes further development, whereas the sodium-implanted titanium surface becomes smoother. This observation can be confirmed statistically by the results of the roughness analysis (Fig. 4).

Examination of bioactivity indicates that, during the first 7 days of exposure, islands of precipitated phosphates of μ-metric dimensions (Fig. 8a) take shape on the surface of the specimens, along with more discreet changes on a nanometric scale (Fig. 3). A prolongation of the exposure in SBF results in an increase in the quantity of precipitates of calcium phosphates on the surface of the specimen, which, after 2,100 h of exposure, form a continuous layer (Fig. 8c). The resulting layers of the calcium phosphate have differing structure and differing proportions of calcium to phosphorus depending on the type of original surface. On a polished

(non-modified) titanium surface, the calcium phosphates do not form a dense layer (Fig. 9a) but, rather, a precipitated one. On the surface of the sodium-implanted titanium specimens, however, the calcium phosphates do form dense layers (Fig. 9b). In Fig. 9 we can see the difference in the behavior of the layers when subjected to the Rockwell hardness test. The phosphate layer on the non-implanted titanium has been pressed flat by the indenter (Fig. 9a), while the dense ceramic phosphate layer on the sodium-implanted specimen has been cracked (Fig. 9b).

The [Ca]/[P] ratio is better for phosphates that form on the sodium-implanted surfaces after both short and long periods of exposure and is equal to about 1.7 (1.66 for hydroxyapatite). The [Ca]/[P] ratio for phosphates that form on the non-implanted surfaces is about 2 and is characteristic for calcium phosphate (Tetra-Ca-phosphate), whose chemical formula is $Ca_4(PO_4)O$).

The cytocompatibility of the sodium-implanted titanium was investigated in vitro. As regards the viability of the cells and their ability to spread on the investigated surfaces, no significant differences were found between modified and unmodified titanium. On the basis of these findings, it can be concluded that sodium-ion implantation does not reduce the titanium's biocompatibility at the cellular level. These results are in alignment with the results of the investigations of Matiz et al. [11].

As regards corrosion resistance, bioactivity, and biocompatibility, our investigations indicate that the optimal sodium dose is 1×10^{17} Na^+/cm^2.

5 Conclusion

1. Sodium-ion implantation produces improved corrosion resistance of titanium after short term exposure.
2. Changes in corrosion resistance during exposure in SBF are a function of the implanted sodium dose. The corrosion resistance of specimens implanted with a dose of 1×10^{17} Na^+/cm^2 remains the same regardless of the length of exposure time, but the corrosion resistance of specimens implanted with a dose of 4×10^{17} Na^+/cm^2 decreases after long exposure in SBF.
3. Sodium-ion implantation produces increased bioactivity and does not reduce the biocompatibility of titanium.

Acknowledgement The authors acknowledge the support of the State Comitte for Scientific Research through the Grant no. 3 T08C 020 26.

References

1. T. Kokubo, S. Ito, Z.T. Huang, T. Hayashi, S. Sakka, T. Kitsugi, J. Biomed. Mater. Res. **24**, 331 (1990)
2. T. Hanawa, M. Ota, Biomaterals. **12**, 767 (1991)
3. T. Kokubo, F. Miyaji, H.-M. Kim, J. Am. Ceram. Soc. **79**, 1127 (1996)
4. H.-M. Kim, F. Miyaji, T. Kokubo, T. Nakamura, J. Biomed. Mater. Res. **32**, 409 (1996)
5. M.T. Pham, W. Matz, H. Reuther, E. Richter, G. Steiner, J. Mater. Sci. Lett. **19**, 1029 (2000)
6. M.T. Pham, W. Matz, D. Grambole, F. Herrmann, H. Reuther, E. Richter, G. Steiner, J. Biomed. Mater. Res. **59**, 716 (2002)
7. M.T. Pham, M.F. Matiz, D. Grambole, F. Herrmann, H. Reuther, E. Richter, J. Mater. Sci. Lett. 20, 295 (2001)
8. K. Cai, J. Brozek, M. Müller, F. Schrempel, J. Bossert, K.D. Jandt, 18th European Conference on Biomaterials, October 1–4, 2003, Stuttgart, Germany
9. M.F. Matiz, M.T. Pham, W. Matz, H. Reuther, G. Steiner, Surf. Coat. Technol. **158–159**, 151 (2002)
10. M.F. Matiz, M.T. Pham, W. Matz, H. Reuther, G. Steiner, E. Richter, Biomol. Eng. **19**, 269 (2002)
11. M.F. Matiz, R.W.Y. Poon, X.Y. Liu, M.T. Pham, P.K. Chu, Biomaterials **26**, 5465 (2005)
12. T. Hanawa, K. Asaoka, H. Ukai, K. Murakami, in *Proceedings of the Symposium of Compatibility of Biomedical Implants* (San Francisco 1994), p. 126
13. T. Hanawa, H. Ukai, K. Murakami, K. Asaoka, Mater. Trans. JIM **36**, 438 (1995)
14. T. Hanawa, Y. Kamiura, T. Lohgo, J. Biomed. Mater. Res. **36**, 131 (1997)
15. D. Krupa, J. Baszkiewicz, J.A. Kozubowski, A. Barcz, J.W. Sobczak, A. Biliński, M. Lewandowska-Szumieł, B. Rajchel, Biomaterials **22**, 2139 (2001)
16. J.G. Zegler, J.P. Biersack, *The Stopping and Range of Ions in Solids Software "Trim-92"* (Pergamon Press, New York, 1985)
17. B.A. Boukamp, *Equivalent Circuit-EQUIVCRT Manual* (Technical University of Twente, 1989)
18. D. Krupa, J. Baszkiewicz, B. Rajchel, A. Barcz, J.W. Sobczak, A. Biliński, Vacuum **78**, 161 (2005)
19. T.P. Hoar, D.C. Mears, Proc. Roy. Soc. London A. **294**, 486 (1966)
20. T. Massalski, editor in-chief "Binary alloy phase diagrams" ASM—International The Materials Information Society Publisher William W. Scott Jr. USA 1990
21. M.T. Pham, M.F. Maitz, W. Matz, H. Reuther, E. Richter, G. Steiner, Thin Solid Films **379**, 50 (2000)
22. R. Lange, F. Lüthen, U. Beck, J. Rychly, A. Baumann, B. Nebe, Biomol. Eng. **19**, 255 (2002)
23. A. Kirbs, R. Lange, B. Nebe, J. Rychly, P. Müller, U. Beck, Mater. Sci. Eng. **C23**, 413 (2003)
24. A. Kirbs, R. Lange, B. Nebe, J. Rychly, A. Bauman, H.G. Neumann, U. Beck, Mater. Sci. Eng. **C23**, 425 (2003)
25. T. Kulik, J. Baszkiewicz, M. Kamiński, J. Latuszkiewicz, M. Matyja, Corr. Sci. **19**, 1001 (1979)
26. J. Baszkiewicz, J.A. Kozubowski, D. Krupa, M. Kamiński, A. Barcz, G. Gawlik, J. Jagielski, J. Mater. Sci. **33**, 4561 (1998)
27. J. Baszkiewicz, M. Kamiński, J.A. Kozubowski, D. Krupa, K. Gosiewska, A. Barcz, G. Gawlik, J. Jagielski, J. Mater. Sci. **35**, 767 (2000)
28. D. Krupa, J. Baszkiewicz, J.A. Kozubowski, A. Barcz, J.W. Sobczak, A. Biliński, M. Lewandowska-Szumieł, B. Rajchel, Biomaterials **23**, 3329 (2002)
29. D. Krupa, J. Baszkiewicz, J.A. Kozubowski, A. Barcz, J.W. Sobczak, A. Biliński, M. Lewandowska-Szumieł, B. Rajchel, Biomaterials **26**, 2847 (2005)
30. X. Wen, X. Wang, N. Zhang, Bio.-Med. Mater. Eng. **6**, 173 (1996)